Experimental report

20/01/2022

Proposal:	**9-10-1698**	**Council:**	10/2020
Title:	Microemulsions in hydrophobic deepeutectic solvents		
Research area:	Chemistry		

This proposal is a new proposal

Main proposer:	**Karen EDLER**
Experimental team:	Ralf SCHWEINS
Local contacts:	Ralf SCHWEINS

Samples:

menthol:C12OOH, AOT, D2O
menthol:C6OOH, AOT, D2O
menthol:d-C6OOH, DDAB, D2O
menthol:d-C10OOH, DDAB, D2O
menthol:C10OOH, AOT, D2O
menthol:d-C12OOH, AOT, D2O

Instrument	Requested days	Allocated days	From	To
D33	2	0		
D11	2	0		
D22	2	1	24/05/2021	25/05/2021

Abstract:

Deep eutectic solvents (DES) are novel hydrogen bonded liquids which support amphiphile self-assembly. DES can be prepared from a wide range of components, which are non-toxic, cheap and from sustainable sources and are of interest for replacing standard organic solvents in a range of applications, including templating and encapsulation/release of active species. Here we wish to investigate their effect on the properties of water-in-oil microemulsions, where the DES acts as the oil phase. The emulsions are stabilised with double chain cationic or anionic surfactants and we aim to determine how the solvent components interact with the stabilising surfactant layer between the oil and water phases, and thus affect the water phase connectivity within the emulsion.

Objectives:

This experiment aimed to examine the structure of water-in-oil (w/o) microemulsions in hydrophobic deep eutectic solvents (DES) composed of mixtures of ʟ-menthol with natural carboxylic acids. DES composed of ʟ-menthol with a carboxylic acid were chosen because, in contrast with many previously well-researched DES, they are water-immiscible and can solubilise hydrophobic species. Moreover, the eutectic phase diagrams and a characterisation of physical properties for this series of DES have also been reported[1]. Three DES from this series were the focus of study for this experiment, namely, those formed of ʟ-menthol with the components hexanoic acid (C_6), decanoic acid (C_{10}), and dodecanoic acid (C_{12}), respectively. Each DES was prepared at a molar ratio of 2:1 ʟ-menthol:acid, to match the eutectic ratio of the ʟ-menthol:dodecanoic acid mixture and to eliminate compositional effects when observing the SANS of DES formed with different components.

Emulsions were prepared using these DES as the oily phase, with the double-tailed surfactants docusate sodium salt (also known as Aerosol OT) (AOT), and didodecyldimethylammonium bromide (DDAB), which facilitate the formation of w/o emulsions, as anionic and cationic surfactants, respectively. D_2O was used for all emulsions in order to provide the strongest contrast in neutron scattering length density, and both protonated and deuterated carboxylic acid components (*h*- and *d*- C_6, C_{10} and C_{12}) were used to provide two different contrasts for the solvent (DES). Due to the lack of commercial availability of deuterated AOT, DDAB, or ʟ-menthol, further contrasts were not available for this experiment.

By examining the SANS from w/o emulsions in different DES from the ʟ-menthol:carboxylic acid series, at different water loadings, it is intended to identify the structures formed therein – hypothesised to be either inverse micelles[2], or a dynamic two-phase structure with a typical correlation length and domain size[3]. By changing the contrast of the carboxylic acid component in the DES mixture, it is also hoped that we can identify whether the formation of an emulsion interacts with the DES structure itself and whether or not the amphiphilic carboxylic acid component can act (partially) as a co-surfactant alongside the added AOT and DDAB species[4,5].

Experimental:

AOT emulsions were prepared at 33wt% in three separate ʟ-menthol:carboxylic acid (2:1) DES, herein referred to as MC6, MC10, and MC12. Additionally, DDAB emulsions were prepared at 33wt% in two separate DES, MC6 and MC10. Once the emulsions had been prepared, samples with different water loadings were prepared by adding D_2O to 0.50 g samples of dry emulsions in different amounts: for 33wt% AOT emulsions; 10 µL (W=1.47), 25 µL (W=3.66), and 40 µL (W=5.86); for DDAB emulsions; 10 µL (W=1.52), 20 µL (W=3.05), and 30 µL (W=4.57).

SANS was measured for samples in quartz glass Hellma cells on the D22 beamline at the ILL, for a total of 46 different samples (3 neat DES, 4 AOT emulsions (dry plus three water loadings) each for 3 DES, 4 DDAB emulsions (dry plus three water loadings) each for two DES, all at two contrasts. All measurements on the beamline were conducted on our behalf by our local contact Dr. Ralf Schweins, to whom we are very grateful, due to our inability to travel to the ILL site because of travel restrictions in the Covid-19 pandemic. All samples were measured in a Q range of 0.0042 $Å^{-1}$ to 0.66 $Å^{-1}$. All neat DES and AOT emulsions remain liquid at room temperature (25 °C) and were measured as such. For DDAB emulsions in MC6, samples were also liquid and measured at 25 °C, however for DDAB emulsions in MC10, measurement at higher temperatures was necessary in order to prevent crystallisation – 40 °C for the dry emulsion and lower water loading (10 µL or W=1.52) and 30 °C for the higher water loadings (20 µL or W=3.05, and 30 µL or W=4.57).

Results:

Example SANS patterns for different water loadings in the MC10_AOT emulsions are shown in **Figure 1a** (hh solvent) and **Figure 1b** (hd solvent). SANS for the AOT emulsions in other MCX DES are broadly similar. For D_2O emulsions in the hh-solvent, a peak can be observed at high Q, which shifts to lower Q and increases in intensity as the water-loading increases. The shapes of these scattering curves are fitted well by a model of spheres with a hard sphere structure factor (fits are shown as solid red lines in **Figure 1a**).

For D_2O emulsions in the hd-solvent, contrast is lower. A low-intensity peak at high Q can be observed to form at higher water loading (40 µL or W=4.57 and 25 µL or W=3.66), however the intensity is too low to discern useful structures for the samples with a lower water loading (the 'dry' or 0 µL AOT emulsion, and the 10 µL or W=1.47 emulsion). Features may become visible upon fitting the non-solvent-background-subtracted data with a summed model, which combines the SANS of the neat DES with the SANS of structures which occur when a w/o emulsion is formed within these DES.

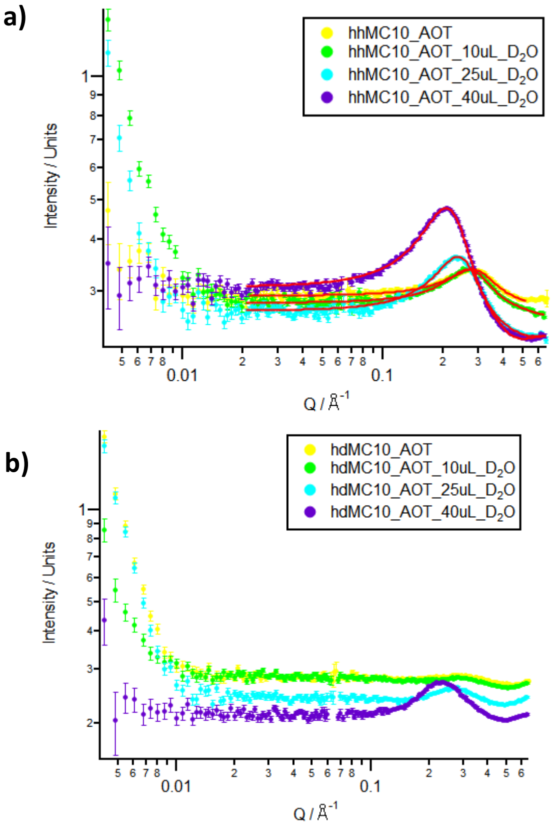

***Figure 1**: SANS for the MC10_AOT microemulsions, for **a)** the hh-MC10 solvent contrast and **b)** the hd-MC10 solvent contrast. Absolute water loadings (µL) refer to amounts added to 0.50 g samples of 33wt% AOT solutions in MC10 DES.*

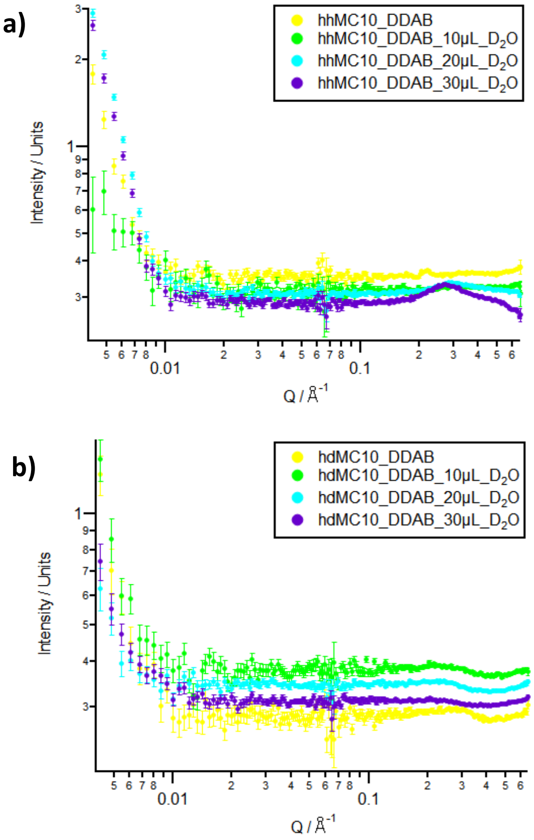

***Figure 1**: SANS for the MC10_DDAB microemulsions, for **a)** the hh-MC10 solvent contrast and **b)** the hd-MC10 solvent contrast. Absolute water loadings (µL) refer to amounts added to 0.50 g samples of 33wt% DDAB solutions in MC10 DES.*

Example SANS patterns for different water loadings in the DDAB emulsions are shown in **Figure 2a** (hh solvent) and **Figure 2b** (hd solvent). In both cases there is little contrast. In the hh-solvent, a very low intensity peak becomes identifiable at the 30 µL or W=4.57 loading, however its low intensity relative to the background somewhat disguises its distinguishing features. In the hd-solvent, D_2O DDAB emulsions show few SANS features in the solvent-background-subtracted data which is presented here, since absolute intensity data from these systems is virtually identical to that of the neat hd-MC10 DES – *i.e.* a characteristic decay in intensity at higher Q (not presented here). These features will be better fitted with a correlation length model, suggesting that inverse micelles do not form when using DDAB as a surfactant. This is to be expected since DDAB has a lower packing parameter of 0.62[6], in comparison with AOT (greater than 1 due to its features leading to a high packing parameter)[7]. However, the peak in the SANS for the dataset hhMC10_DDAB_30µL_D_2O (**Figure 2a**) may suggest a change in structure at the 30 µL or W=4.57 loading, the highest water loading possible (in steps of 10 µL) before the microemulsion system became turbid and cloudy indicating a macroscopic phase separation.

Conclusions:

Structural analysis of the data and fitting to suitable models is ongoing using the software SasView 5.0.3. The data will contribute towards the PhD thesis of Jake Hooton and a publication is expected. Further evidence to support the arguments made during data fitting will be provided in the form of SAXS measured from the same sample on an in-house instrument. Further proposals to a SANS facility for either another experiment or rapid access samples may also follow.

References:

1 M. A. R. Martins, E. A. Crespo, P. V. A. Pontes, L. P. Silva, M. Bülow, G. J. Maximo, E. A. C. Batista, C. Held, S. P. Pinho and J. A. P. Coutinho, *ACS Sustain. Chem. Eng.*, 2018, **6**, 8836–8846.
2 S. Nave, J. Eastoe, R. K. Heenan, D. Steytler and I. Grillo, *Langmuir*, 2000, **16**, 8741–8748.
3 C. P. Cabry, L. D'Andrea, K. Shimizu, I. Grillo, P. Li, S. Rogers, D. W. Bruce, J. N. Canongia Lopes and J. M. Slattery, *Faraday Discuss.*, 2018, **206**, 265–289.
4 S. Ray and S. P. Moulik, *J. Colloid Interface Sci.*, 1995, **173**, 28–33.
5 S. Prevost, T. Lopian, M. Pleines, O. Diat and T. Zemb, *J. Appl. Crystallogr.*, 2016, **49**, 2063–2072.
6 G. G. Warr, R. Sen, D. Fennell Evans and J. E. Trend, *J. Phys. Chem.*, 1988, **92**, 774–783.
7 B. Simmons, V. Agarwal, G. McPherson, V. John and A. Bose, *Langmuir*, 2002, **18**, 8345–8349.